Chapter 10

Mechanical Characterization of Rigid PUR Foams Used for Wind Turbine Blades Construction

Emanoil Linul[*1], Liviu Marsavina[2]

[1,2]Mechanics and Strength of Materials Department, Politehnica University of Timisoara
1 Mihai Viteazu Avenue, Romania

[*1]linul_emanoil@yahoo.com; [2]lmarsavina@yahoo.com

I. INTRODUCTION

The design and structural reliability of advanced materials like composites and sandwich materials require a better understanding of how the fracture process initiates and progresses to final failure. The sandwich structural concept consists of two (or more) thin, stiff, strong and relatively dense faces sheets which are bonded to a thick and low density core. This structural assembly offers superior specific flexural stiffness and strength. To this end, advanced composite sandwich structures have been widely used in aerospace structures, marine industry, automobiles, wind turbine blades, pipelines, bridge decks, etc. due to their superior structural capacity in carrying transverse loads with minimal weight penalty [1-3].

Most wind turbines have the same basic parts: blades, shafts, gears, generator and a cable (some turbines do not have gearboxes). These components work together to convert the wind energy into electricity. As we know wind turbines capture most of energy depending on the size of their propellers (i.e., blades). So, the blades are the most important critical parts of wind turbine [4]. The thin sheets (glass fiber reinforced composites – GFRP, carbon fiber reinforced composites – CFRP, etc.) which forms the shell of the wind blade, although may be mechanically strong enough to endure the loads but as a whole structure it is not stiff enough and would undergo large deflection under wind loads. In order to obtain a deflection as small as possible and adequate stiffness of composite sandwich structure requires the correct choice of the core material, so the blade can effectively endure the loads. Types of foams that can be suitably used as cores for wind blades structures are as follows: polyvinyl chloride (PVC) foam, polystyrene (PS) foam and polyurethane (PUR) foam [5].

In order to obtain a greater efficiency of energy capture, there has been a dramatic increase in the size and power output of wind turbines during the past 20 – 30 years, from a rated power of 50 kW to multi – megawatt (≈ 5 – 7 MW) power plants of today (see Fig. 1). The wind industry is focused on developing longer blades that take advantage of recent developments in the field of composite technology to increase wind turbine energy output without adding excessive weight or sacrificing essential strength. It is anticipated that wind turbines with a rated power output in the range of 8 – 10 MW and a rotor diameter from 180 – 200 m will be developed and installed within the next 10 – 15 years [4].

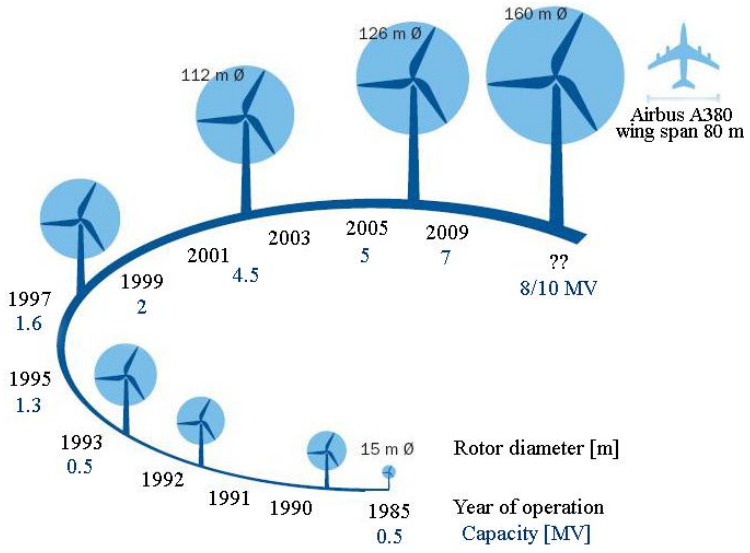

Fig. 1 Size evolution of wind turbine blades

This trend to perform longer blades brings with it a new engineering challenge, notably: creating blades that are both strong and light in weight. While weight increases with the sheer size of the blade, structural modifications necessary to increase the blade strength – to stand up to the added forces generated by rotation of the larger blades – can add even more weight. With the lack of proper attention to weight savings in the design and fabrication of large blades, raw material costs and fabrication cycle times can increase excessively. But heavy blades are also a problem in the field where greater stress concentrations may be developed on wind turbine bearing sets. In addition, most importantly, extra weight imposes a much higher fatigue penalty during wind turbine operation, which shortens the blade lifetime. One approach to reduce the blade mass and the resulting weight is to use more carbon fiber in composite lay-ups, but this can increase material expense considerably. Another potentially more promising route to reducing mass and controlling blade weight are improvements in foam core properties, resin systems and skin/core bonding. Advances achieved in these areas can reduce the blade mass, extend its entire life and lower the fabrication cycle time and the associated cost.

Several studies have been carried out and many analytical/numerical models have been performed in order to investigate the mechanical behavior of the wind turbine blades [6-10]. The aerodynamic properties of a wind turbine airfoil were investigated by Sicot et al. [6], focusing particularly on stall mechanisms. Also, a method to determine the position of the separation point and the value of the chordwise pressure gradient in the separated area has been proposed. They have shown that, for the same angle of attack, the separation point is nearer to the trailing edge when the inflow turbulence level increases (a stall delay). Likewise, the fatigue life for operating more than 20 years was estimated by Kong et al. [7] using (i) the well – known S-N linear damage equation, (ii) the load spectrum and (iii) Spera's empirical formulae. Furthermore, a study with a discussion concerned with an actual collapse testing under the flap – wise loading for a large full – scale composite wind turbine blade was conducted by Yang et al. [8] to assess and evaluate the structural response of the blade during loading and after collapse by correlating experimental results with numerical model predictions. A technique of videometrics was adopted to measure the integral deformation and the local deformation of the wind turbine blade under the flap – wise loading. Another study of prismatic composite I-beams, designed within the UpWind – project to examine the mechanical behavior of adhesive bond lines, were numerically and experimentally investigated by Zarouchas et al. [9]. The results of the simulation were directly compared with the experimental observations coming from Digital Image Correlation Technique (DICT) and conventional techniques (Linear Variable Differential Transformers – LVDT and strain gages). On the other hand, Yang and Sun [4] have undertaken studies on the testing, inspecting and monitoring technologies for wind turbine blades, including mechanical property testing, non – destructive testing/inspecting, full – scale testing, structural health monitoring and condition monitoring. And then, the development trends and some suggestions of testing, inspecting and monitoring technologies for wind turbine blades were fully discussed. In addition, the progressive failure process of composite sandwich wind turbine blades subjected to wind load was studied via both theoretical and experimental approaches by Chen and Kam [10]. In the theoretical study, the wind pressure acting on the wind blade surface was estimated on the basis of an aerodynamic analysis. Whereas, in the experimental investigation, a composite sandwich wind blade was fabricated for the purpose of strength testing.

In this context, a variety of synthetic polymer foams and different wood sorts are used as core materials in the sandwich blade structures. Fig. 2 presents a cross section through a wind turbine blade after Yang et al. [8].

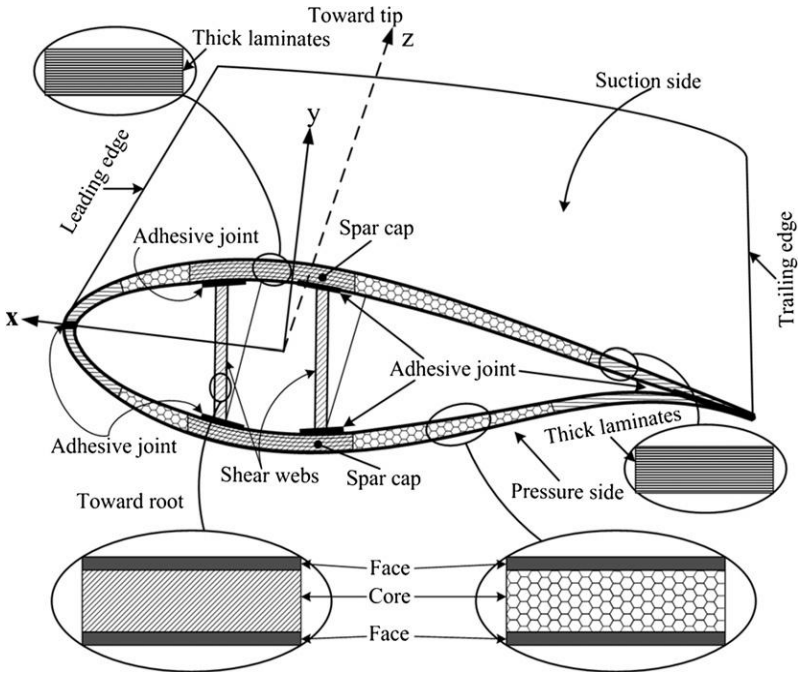

Fig. 2 Cross-section through a wind turbine blade after Yang et al. [8]

Since sandwich structures are manufactured by different methods such as: (i) resin transfer moulding, (ii) compression moulding and (iii) autoclave vacuum bag moulding, two important factors are frequently overlooked [11]: (1) the bonding between the face and core of sandwich structures is assumed to be perfect bonding and (2) in many cases the manufacturing parameters of the sandwich structures are selected as the same as those of the composite faces [12].

Mechanical property testing is usually carried out on coupons and subcomponents with a representative lay – up and a similar processing way to that of the blade in question. Mechanical properties are measured under tensile, compressive and shear loads, or combinations thereof, which mainly include static testing, fatigue testing and modal testing. The purpose of static testing is to verify the capacity of sustaining limit load [4]. The prediction of this type of damage has attracted much interest since such an attainment would increase the confidence on the design of sandwich structures and subsequently expand their field of application. There is a high demand for these materials to withstand both static and dynamic loads without the risk of brittle fracture.

This work aims to provide a better understanding of the failure mechanisms in wind turbine blade with the focus on the core materials (rigid polyurethane foams). In this respect we will make a mechanical characterization of rigid PUR foams under different loading conditions. This characterization of selected cores will be done through static and dynamic tests using different densities, loading speed, temperature and different loading plans according to the core forming plan. This investigation has to be done because as it can be seen from Fig. 3 that faces/core material of a sandwich beam/panel can fail in several ways: (i) it may fail by the yielding or fracture of the faces (as shown in Fig. 3b); (ii) the compression face may "wrinkle" or "dimple" (as shown in Fig. 3c); (iii) the core can fail, usually in shear (as shown in Fig. 3d). However, compression and tensile failures or local crushing can also occur. Further to that, the bond between the face and the core can also fail; and since resin adhesives are usually brittle, debonding may occur by brittle fracture (as shown in Fig. 3e). As a final point, the sandwich can fail by indentation of the faces and core at the loading point [1, 2]. These material properties are critical in the structural performance of the foam core of wind turbine blade.

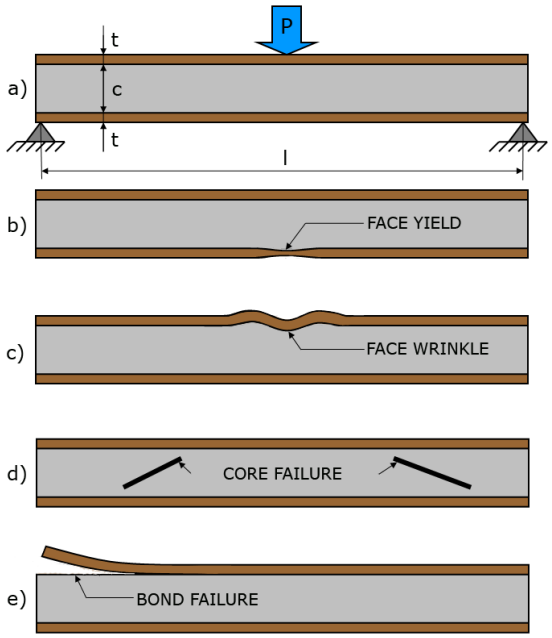

Fig. 3 Failure modes of sandwich beams or panels

The initiation, propagation and interaction of failure modes depend on the type of loading, constituent of material properties and geometrical dimensions. The experimental program was specifically designed according to the aim of the work. Considering the types of loading and types of foam, the following aspects have been analyzed: determination of mechanical characteristics in static and dynamic compression tests and determination of fracture toughness both under static and dynamic regime on notched specimens. Finally, at the end of the section, a microstructural analysis was presented for specimens both before and after deformation.

II. STATIC AND DYNAMIC COMPRESSION TESTS

Research on characterization of cellular materials under compressive loading conditions has been widely reported as in [13–16]. The various properties and attributes investigated include energy absorption, density, cell structure, yield criteria, strain rate, energy efficiency, etc. Avalle at al. [13] have presented an optimization procedure in order to identify the micromechanical parameters from uniaxial compression test of different types of foams. The effect of the density and filler size was also investigated in [14]. Ramsteiner et al. [17] have analyzed the parameters influencing the mechanical properties of foam. The parameters that were identified and studied are the following: the structure of the foam, the matrix material of the

foam, the density of the foam, cell orientation and testing temperature. Linul et al. [18] have presented a comparison, of stress-strain response in compression, between experimental results and micromechanical modeling for PUR foams. The crush behavior of Rohacell structural foam was investigated by Li et al. [19]. Tu et al. [20] presented the plastic deformations of PUR foam under static compressive loading and proposed a theoretical approach to describe the deformation localization.

The mechanical behavior of rigid polyurethane foams under compressive loading is probably the primary property that distinguishes it from non-cellular solids. The use of foams in kinetic energy absorption and structural applications, whereby they are subjected to static and dynamic loading, motivates the need to study their mechanical properties [21].

A. Static Compression Tests of Rigid PUR Foam

This study presents the determination of the main mechanical properties of polyurethane foam in static compression. The influence of density, loading speed effect and forming plane on mechanical properties were investigated. The main parameters studied in compression include: Young's modulus, yield stress, plateau stress and densification strain; defined as follows (see Fig. 4):

- Young's modulus, E [MPa] – the ratio of stress (nominal) to corresponding strain below the proportional limit of a material expressed in force per unit area based on the minimum initial cross-sectional area [22].
- Compressive yield point, σ_y [MPa] – the first point on the stress-strain diagram at which an increase in strain occurs without an increase in stress [22].
- Plateau stress, σ_{pl} [MPa] – constant stress when strain increases [1, 20]. For many types of rigid PU foams, the plateau regime starts from the crush strain, ε_y, or crush stress, σ_y, representing the initiation of the new deformation mechanism of the cell wall or the cell wall failure, and ends at a critical strain, ε_D, representing the onset of densification [19].

The onset strain of densification can be determinates by several methods [19]:

- Method I – The onset strain of densification is defined by the intersection of the tangents to the stress plateau regime and the densification regime [23-25].

- Method II – The onset of densification is defined as the strain at the local minimum before the stress rises steeply [26].

- Method III – The onset strain of densification is defined as the strain at which the slope of the tangent is equal to that of the elastic regime [25].

- Method IV – Li et al. [19], suggest using the energy efficiency expressed by Eq. (1). The onset strain of densification is defined as the strain at which the slope of the curve in a plot of energy efficiency (η) versus strain (ε) is zero, Eq. (2) [27].

$$\eta(\varepsilon) = \frac{1}{\sigma(\varepsilon)} \cdot \int_0^{\varepsilon} \sigma(\varepsilon) \cdot d\varepsilon \tag{1}$$

$$\left. \frac{d\eta(\varepsilon)}{d\varepsilon} \right|_{\varepsilon=\varepsilon_D} = 0 \tag{2}$$

Based on the experimental data the energy efficiency (according to Eq. (1)) is plotted in Fig. 5 for rigid polyurethane foams with densities of 40, 80 and 200 kg/m3, and the onset strain of densification is determined according to Eq. (2).

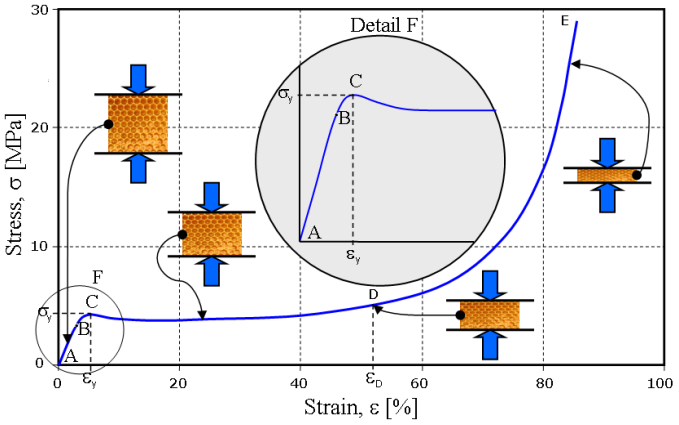

Fig. 4 Typical stress – strain curve for rigid polyurethane foam

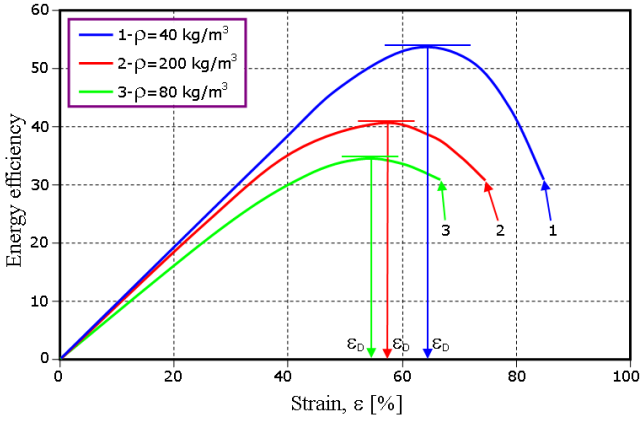

Fig. 5 Energy efficiency-strain curves for three different densities

The specimens used for experimental tests were in the form of cubes [14, 28]. Shapes of used specimens are shown in Fig. 6, in the same figure are presented: comparisons between the initial shapes (before test) and final shapes (after test) of the specimen [18].

Experimental tests were performed on a Walter Bay 10 kN testing machine (Fig. 7a) at room temperature. The samples were subjected to a uniaxial compressive loading at a speed of 2 mm/min, except for samples that are used for determining the effect of loading speed, where 1; 5; 10 and 20 mm/min were used. Figure 7b shows the positioning of the specimen. For each type of test, 5 specimens were used and the tests were performed in accordance with ASTM D1621 – 00 Standard Test Method for Compressive Properties of Rigid Cellular Plastics [22]. Also, it should be pointed out that specimens have to be placed on the centre of the plates.

Fig. 6 Compression specimens used in the experimental program

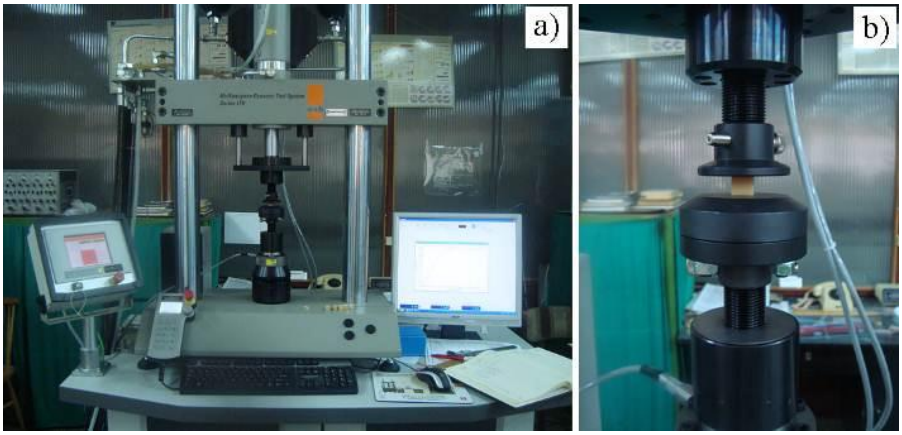

Fig. 7 A Walter Bay 10 kN testing machine

Fig. 8 presents typical stress – strain curves for different densities, showing an increase of mechanical properties with increasing density. Mean values of these properties as a function of density and loading speed are listed in Table 1 and 2.

Figs. 9 and 10 presents the influence of loading speed and effect of loading direction, respectively on compressive behavior of 140 kg/m3 closed – cell PUR foams. For the in – plane loading direction a constant plateau was obtained, while for out – of – plane load the plateau has a linear hardening for the same foam density.

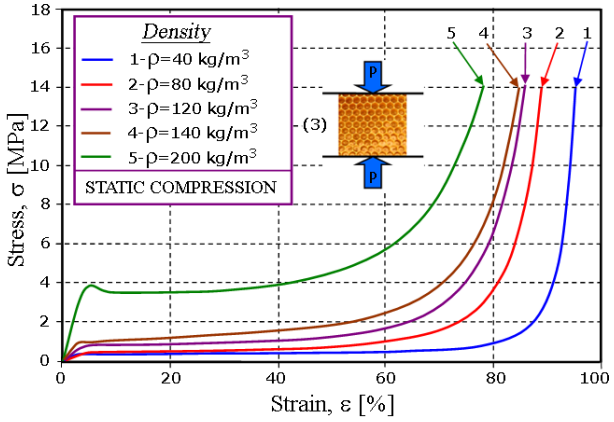

Fig. 8 Typical stress-strain curves in compression. Effect of density

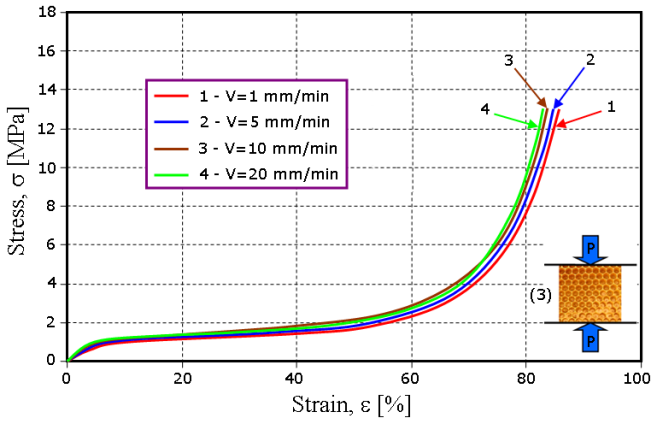

Fig. 9 As Fig. 8 in compression. Effect of loading speed

TABLE 1 MEAN VALUES OF MECHANICAL PROPERTIES FOR STATIC COMPRESSION AS A FUNCTION OF DENSITY

Density [kg/m^3]	Geometrical parameters			Loading direction	Young's Modulus [MPa]	Yield Stress [MPa]	Plateau Stress [MPa]	Densification [%]
	h [mm]	b_1 [mm]	b_2 [mm]					
40	12.78	12.78	12.66	(3)	4.20	0.38	0.39	65.53
80	15.08	14.90	14.84		7.90	0.48	0.51	54.57
120	15.42	15.28	15.22		18.37	0.89	0.93	54.31
140	14.02	12.06	12.04		34.11	1.05	1.21	54.47
200	11.76	11.72	11.72		121.99	4.14	3.86	55.75

TABLE 2 MEAN VALUES OF MECHANICAL PROPERTIES FOR STATIC COMPRESSION AS A FUNCTION OF LOADING SPEED

Density [kg/m^3]	Geometrical parameters			Loading speed [mm/min]	Young's Modulus [MPa]	Yield Stress [MPa]	Plateau Stress [MPa]	Densification [%]
	h [mm]	b_1 [mm]	b_2 [mm]					
140	13.2	13.6	13.6	1	18.94	1.01	1.16	50.71
	13.6	13.6	13.8	5	21.67	1.07	1.22	52.17
	13.2	13.4	13.6	10	22.48	1.17	1.30	50.56
	13.4	13.2	13.6	20	25.57	1.22	1.40	53.87

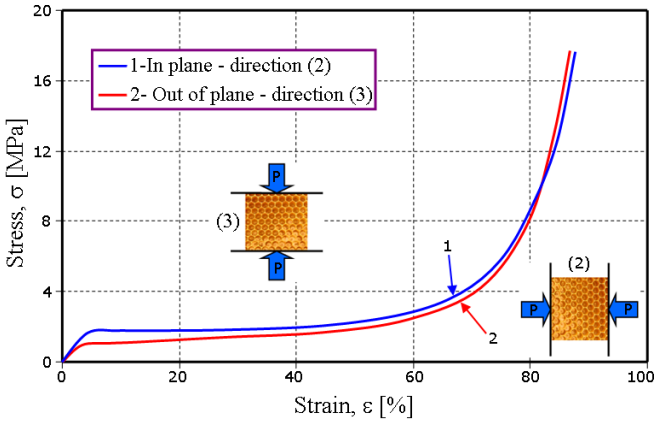

Fig 10 Typical stress-strain curves in compression. Effect of loading direction

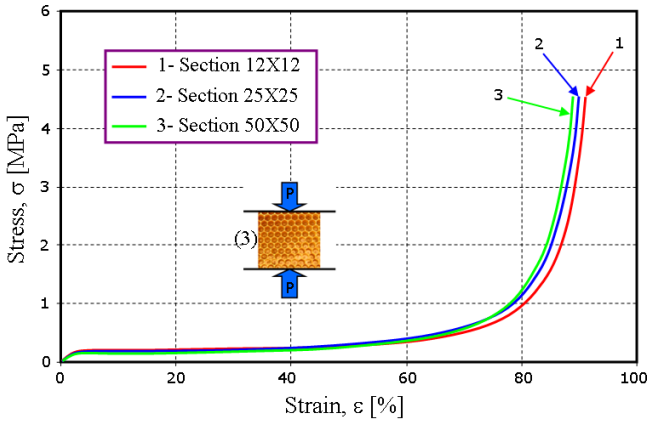

Fig. 11 As Fig. 10 in compression. Effect of cross-section

In Fig. 12 are shown the sampling of the compression specimens extracted from a rectangular SF plate and the two loading directions that were used in the compression tests. In this respect, all tested specimens were cut from the same plate.

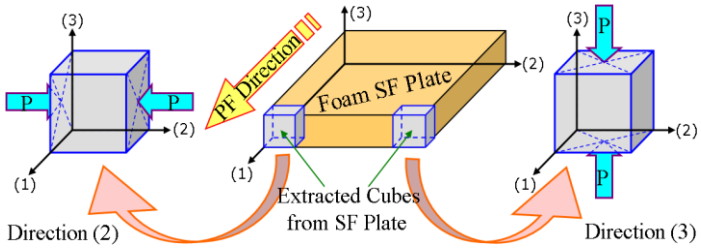

Fig. 12 The sampling of the cube specimens from a rectangular plate

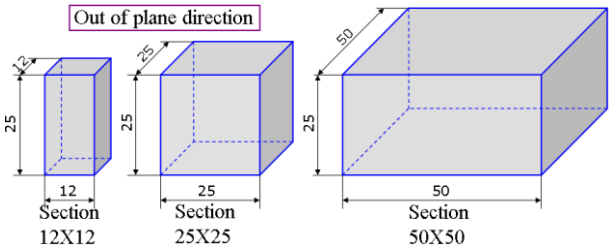

Fig. 13 Shapes used as specimens for cross section study

The shapes and geometrical parameters of specimens for cross section study are shown in Fig. 13; whereas Fig. 11 illustrates typical stress – strain curves. In this case the samples had the same height (h=25 mm), but different values for b_1 and b_2, (12×12, 25×25, 50×50 mm^2, respectively). It is observed from Fig. 11 that the cross – section shows a relatively small influence on the mechanical properties in compression.

As a result of cross – section influence, Table 3 presents the mean values of the mechanical characteristics in static compression for 140 kg/m^3 foam density.

TABLE 3 MEAN VALUES OF MECHANICAL PROPERTIES FOR STATIC COMPRESSION AS A FUNCTION OF CROSS – SECTION

Density [Kg/m^3]	Geometrical parameters			Cross section	Young's Modulus [MPa]	Yield Stress [MPa]	Plateau Stress [MPa]	Densification [%]
	h [mm]	b_1 [mm]	b_2 [mm]					
40	25.0	12.2	12.2	12X12	4.91	0.23	0.24	53.82
	25.2	25.2	25.4	25X25	5.17	0.20	0.21	53.68
	24.8	49.8	50.0	50X50	5.32	0.16	0.18	53.63

B. Dynamic Compression Tests of Rigid PUR Foam

For the characterization of mechanical behavior on dynamic compression loading, rigid PUR foams used in the experimental program correspond to the static compression tests. The specimens used in this case are identical to those used for static compression tests and are shown in Fig. 6. The specimens were subjected to uniaxial dynamic compression with loading speed ranging from 0.62 – 6 m/s, using different temperature scales (i.e., 20, 60 and 100 ℃).

Experimental tests were made in the Strength of Materials Laboratory at Lublin University of Technology, Poland. Tests were carried on a 40 kN Instron – Dynatup impact testing machine as shown in Fig. 14.

Fig. 14 A Instron – Dynatup 40 kN impact testing machine

Mechanical behavior of rigid foams under compression tests was determined in accordance with the ASTM D1621 – 00, Standard Test Method for Compressive Properties of Rigid Cellular Plastics [22].

The following subsection will study in detail the influence of density, loading speed, material orientation and temperature on the mechanical properties of rigid PUR foams that are subjected to dynamic compression loads. Parameters such as Young's modulus, yield stress, plateau stress and densification have a very important role in the real applications of these materials and for this reason the foam behavior will be presented under different loading and temperature conditions.

1) Influence of density

From the data provided by the test machine, the conventional characteristic curves for the tested specimens were plotted. Fig. 15 shows a comparison of typical stress – strain curves for the four densities of rigid PUR foams (i.e., 40; 80; 120 and 140 kg/m^3) that are subjected to dynamic compression. Presented curves are obtained from out – of – plane loading direction at room temperature. Variations of Young's modulus with density for out-of-plane loading direction (direction (3)) are presented in Fig. 16.

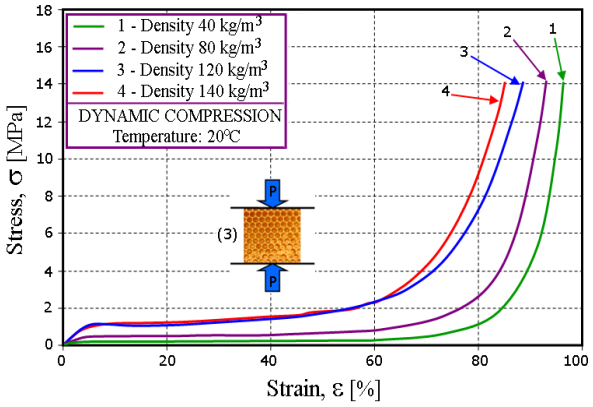

Fig. 15 Typical stress-strain curves. Effect of density

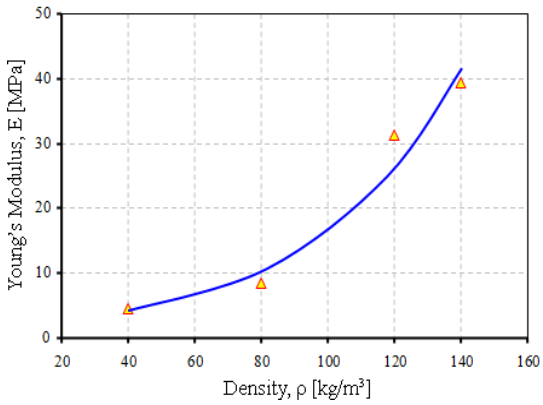

Fig. 16 Young's modulus variation with density. Effect of density

From the recorded stress – strain diagrams, the following regions can be identified: the first part of the curve shows a linear – elastic behavior up to material yield point (up to a strain of 5% approximately), a small softening in stress after yield, a plateau after yield (between 10 – 50%) and in the end there is an increase in stress without a significant increase in strain, commonly known as densification (above 50% strain).

Both Figs. 15 and 16 show a significant increase of mechanical properties (Young's modulus, yield stress and plateau stress) with increasing of density. This means that the density has a major role in determining the mechanical properties in compression. On the other hand, it was found that only densification decreases with increasing of foams density from a value of about 67% to a value of about 57%.

Mean values of mechanical properties for both in-plane (direction (2)) and out-of-plane loading direction (direction (3)), respectively are presented in Table 4 and Table 5.

TABLE 4 MEAN VALUES OF MECHANICAL PROPERTIES ON DYNAMIC COMPRESSION FOR DIRECTION (2)

Density [kg/m^3]	Loading Speed [m/s]	Young's Modulus [MPa]	Yield Stress [MPa]	Plateau Stress [MPa]	Densification [%]
40	0.62	3.89	0.39	0.39	66.02
	0.78	4.12	0.37	0.37	62.86
	0.94	4.50	0.37	0.38	64.89
80	0.78	5.37	0.49	0.48	59.71
	1.09	6.40	0.42	0.42	53.98
	1.28	5.98	0.42	0.43	58.93
120	1.28	33.90	1.53	1.48	58.80
	1.67	31.30	1.72	1.47	54.13
	1.98	32.16	1.73	1.60	57.34
140	0.94	33.10	1.72	1.62	56.88
	1.28	39.43	1.83	1.71	57.60
	1.67	33.47	1.84	1.55	57.12

TABLE 5 MEAN VALUES OF MECHANICAL PROPERTIES ON DYNAMIC COMPRESSION FOR DIRECTION (3)

Density [kg/m^3]	Loading Speed [m/s]	Young's Modulus [MPa]	Yield Stress [MPa]	Plateau Stress [MPa]	Densification [%]
40	0.62	4.49	0.39	0.39	66.77
	0.78	4.04	0.38	0.38	66.07
	0.94	4.49	0.37	0.37	65.13
80	0.78	7.74	0.54	0.54	62.97
	1.09	8.41	0.55	0.53	57.05
	1.28	8.42	0.47	0.49	55.02
120	1.28	24.57	1.17	1.15	59.79
	1.67	26.98	1.12	1.07	57.29
	1.98	26.89	1.10	1.15	58.09
140	0.94	22.37	0.98	1.04	56.98
	1.28	24.82	1.10	1.20	56.91
	1.67	25.62	1.05	1.01	52.89

2) Influence of loading speed

Considering the wide range of applications of cellular materials, it is very important to know how these materials behave in different dynamic loads that can be applied at different speeds. Thus, another important parameter is studied in this chapter, it concerns the influence of loading speed on the mechanical behavior of rigid foams. Fig. 17 shows the influence of the mentioned parameter on the compressive behavior of three different densities 80, 93 and 200 kg/m^3. The specimens were subjected to uniaxial dynamic compression with loading speed within the range of 0.62 – 6 m/s at room temperature of (20 ℃). Figure 18 shows the variation of Young's modulus with loading speed for two different densities (93 and 200 kg/m^3).

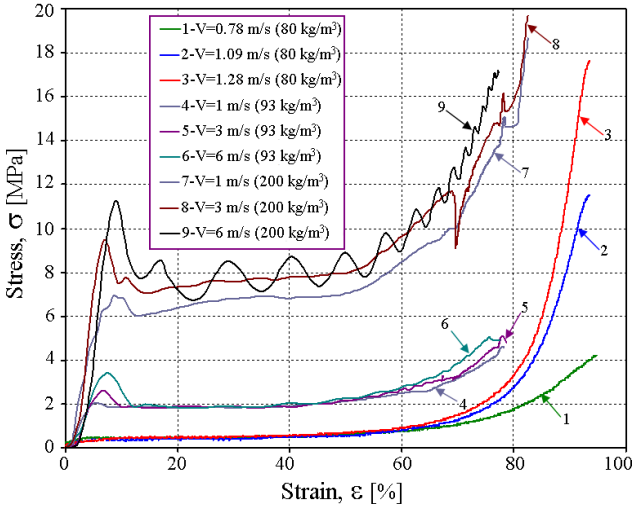

Fig. 17 Stress-strain curves. Effect of loading speed

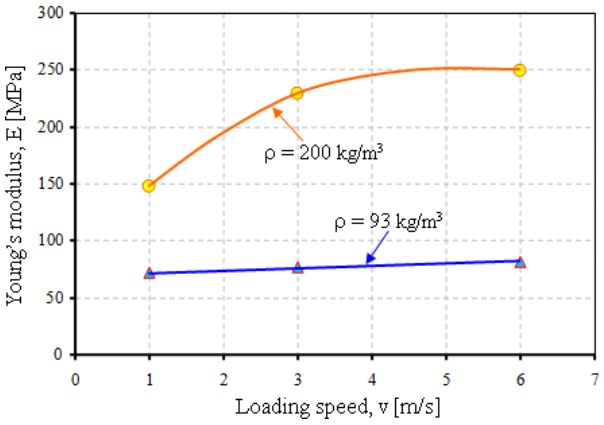

Fig. 18 Young's modulus variation with density. Effect of loading speed

From Figs. 17 and 18 it can easily be seen that the loading speed has a little influence on the mechanical properties in dynamic compression for low density PUR foams (80 and 93 kg/m^3), while for foam with high density (200 kg/m^3), loading speed has a major influence. Also, it can be observed that the biggest influence is obtained for linear-elastic region, yield stress and densification region, while plateau region almost coincide. The yield stress difference between the highest and lowest loading speed is about 1.8 times.

3) Influence of temperature

Considering sudden temperature changes (from one region/country to another) is very important to carrying out a study of the influence of temperature on mechanical behavior of core wind turbine blade. This study was performed for four different rigid PUR foams at three different temperatures: 20, 60 and 100°C and two loading directions (in – plane and out – of – plane). Table 6 recapitulates the mean values of the mechanical characteristics on dynamic compression behavior depending on temperature for the two loading directions.

TABLE 6 MECHANICAL PROPERTIES DEPENDING ON TEMPERATURE

Denity [kg/m^3]	Loading direction	Temperature [℃]	Young Modulus [MPa]	Yield Stress [MPa]	Plateau Stress [MPa]	Densification [%]
40	(2)	60	4.46	0.37	0.37	65.35
		100	21.52	0.24	0.20	62.02
	(3)	60	4.04	0.37	0.37	64.40
		100	16.62	0.39	0.31	64.41
80	(2)	60	8.80	0.50	0.48	54.16
		100	46.50	0.58	0.44	52.10
	(3)	60	55.40	0.62	0.57	53.59
		100	64.72	0.51	0.40	53.51
120	(2)	60	69.80	1.93	1.57	59.09
		100	120.74	1.66	1.30	56.20
	(3)	60	80.48	1.46	1.33	59.43
		100	63.57	1.18	1.10	56.26
140	(2)	60	40.62	1.94	1.71	55.73
		100	50.73	0.78	0.72	56.18
	(3)	60	52.66	1.35	1.35	53.69
		100	12.99	0.58	0.67	54.21

For this purpose and for easier understanding of the behavior, Fig. 19 shows the effect of temperature on the stress-strain curves only for 140 kg/m^3 foam density at 1.67 m/s loading speed; the load has been applied in – plane.

According to the results shown in Fig. 19, it can be seen that at room temperature (20 ℃) and a temperature of 60 ℃, the foam behavior is approximately the same for both cases, while at higher temperatures (100 ℃), the foam behaves differently and changes in its properties are discerned. It should be noted that, for polyurethane foams, the temperature of 100 ℃ is considered to be high because their melting temperature is around 150 ℃.

1) Influence of forming plane

Foam anisotropy is a very important parameter and this should be considered in both practical applications and modeling of the mechanical properties. Thus, choosing the properly of this parameter, we can obtain the desired characteristics for practical applications. Fig. 20 presents the influence of forming plane and loading direction on dynamic compression. In this case, a foam with a density of 140 kg/m^3 at room temperature (20 ℃) and a loading speed v=1.67 m/s was investigated.

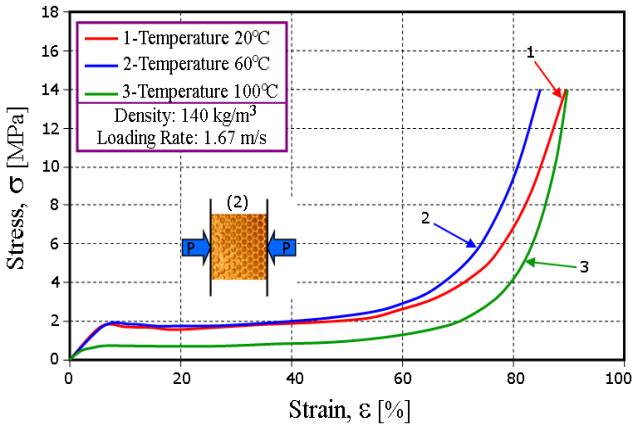

Fig. 19 Stress-strain curves. Effect of temperature

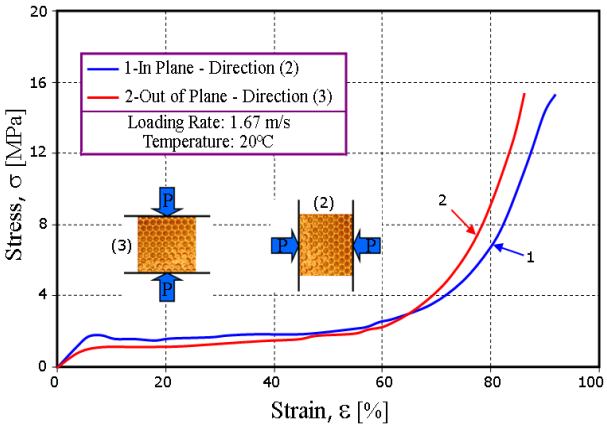

Fig. 20 Stress-strain curves. Effect of forming plane

Loading direction has a significant contribution to the compressive mechanical properties; this aspect highlights the anisotropic behavior of foam. Anisotropy aspect is particularly strong for high – density foam (140 kg/m^3), while in the case of low – density foam (40 kg/m^3) is poor and almost unobservable. In the case of 140 kg/m^3, the material is highly anisotropic, much higher in – plane than out – of – plane, for which the Young's modulus increases from 24.82 MPa to 39.43 MPa, the yield stress increases from 1.10 MPa to 1.83 MPa and the plateau stress increases from 1.20 MPa to 1.71 MPa, while the densification remains the same (approximately 57%) – see Table 4 and 5.

C. Comparison between Static and Dynamic Parameters in Compression

Fig. 21 presents a comparison between stress – strain curves for compressive tests, both in static and dynamic regime. The tests were carried out for several densities, and in Fig. 21 are shown only the results for 140 kg/m^3 density in two loading planes (in – plane and out – of – plane). In this case, the temperature used was 20 ℃ and the loading speed was 2 mm/min ($3.3 \cdot 10^{-5}$ m/s) in static conditions and 1.67 m/s under dynamic conditions.

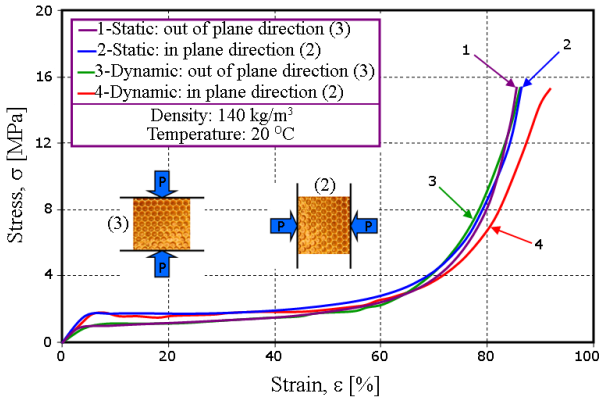

Fig. 21 Stress – strain curves showing a comparison between static and dynamic behavior

As it can be seen from Fig. 21, the behavior under static and dynamic regime of rigid polyurethane foams is almost identical for the applied conditions; the major difference is only between forming planes. According to the results presented in Tables 1, 4, 5 and Figs. 22-25 Young's modulus, yield stress, plateau stress and densification are seen to be dependent on the density. In addition, these diagrams show a comparison between static and dynamic parameters at room temperature [18, 29].

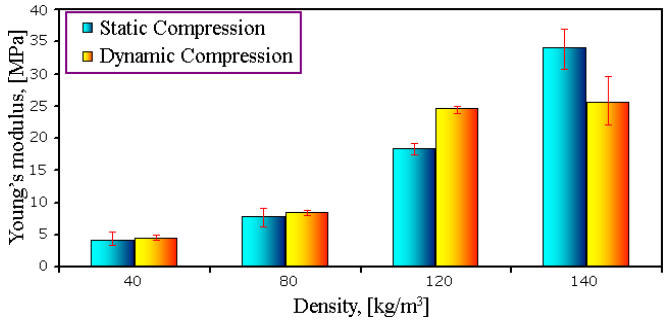

Fig. 22 Young's modulus results versus density. Static – dynamic comparison

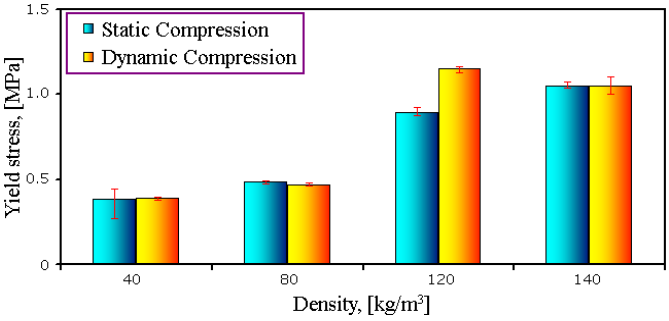

Fig. 23 Yield stress results versus density. Static – dynamic comparison

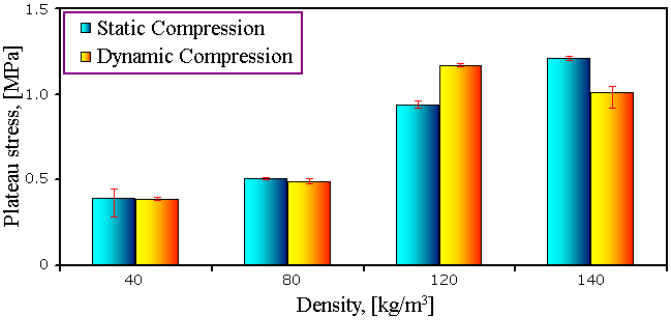

Fig. 24 Plateau stress results versus density. Static – dynamic comparison

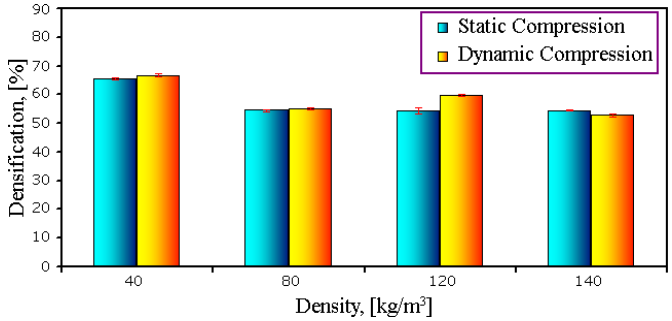

Fig. 25 Densification results versus density. Static – dynamic comparison

III. FRACTURE TOUGHNESS TESTS

Many efforts have been made in recent years to determine the fracture toughness of such foams under static and dynamic loading conditions [30-37]. McIntyre and Anderson [31], have measured the K_{IC} for different densities, using single edge notch specimen, made of rigid closed – cell PU foams for different densities. They found that the fracture toughness is independent of crack length and deduced a linear correlation of K_{IC} with density for foams with densities less than 200 kg/m^3. At higher densities the correlation becomes non – linear. Linear relationship between K_{IC} and density (90-235 kg/m^3), was also obtained by Danielsson [32] for PVC Divinicel HD using three point bending test specimen. Burman [33] presented fracture toughness results for two commercial foams Rohacell WF51 (density 52 kg/m^3) and Dyvinicell H100 (density 100 kg/m^3) using SENB specimens. Vianna and Carlsson [34] presented results of fracture toughness for PVC foams of different densities (36, 80, 100, 200 AND 400 kg/m^3). Kabir and Sasha [35] using 3PB tests have determined fracture toughness for polyvinyl chloride (PVC) and polyurethane (PU) foams. Also, fracture toughness was investigated by Marsavina and Linul [36], and Linul et al. [37] for three different densities of rigid polyurethane (PUR) foams (40, 140 and 200 kg/m^3).

In order to verify that a valid K_{IC} has been determined, it is necessary to first calculate a conditional result, K_Q, which involves a construction on the test record, and then determine whether this result is consistent with the size of the specimen. Fig. 26 presents the force – displacement curve, where the critical load P_Q can be determined.

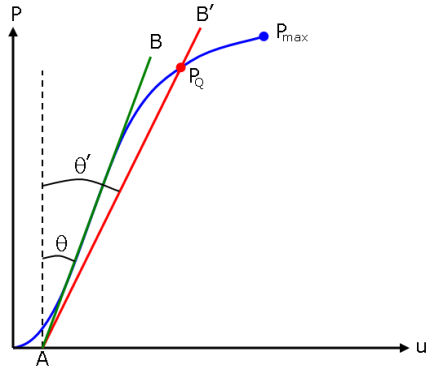

Fig. 26 Force – displacement curve for determining the critical load P_Q

The procedure to determine the critical load is as follows: (i) draw a best straight line (AB) to determine the initial compliance, C ($C=\tan\theta$; $1.05C=\tan\theta'$). C is given by the reciprocal of the slope of line (AB); (ii) draw a second line (AB') with a compliance of 5 % greater than that of line (AB). If the maximum load that the specimen was able to sustain, P_{max}, falls within lines (AB) and (AB'), use P_{max} to calculate K_Q. If P_{max} falls outside line (AB) and line (AB'), then use the intersection of line (AB') and the load curve as P_Q. Furthermore, if $P_{max}/P_Q < 1.1$, use P_Q in the calculation of K_Q. However, if $P_{max}/P_Q > 1.1$, the test is invalid [38].

For a specimen that meets the condition $L/W=4$, K_Q can be determined by the following relation:

$$K_Q = \left(\frac{P_Q}{BW^{1/2}}\right) f\left(\frac{a}{W}\right), \text{ with: } 0 < \frac{a}{W} < 1 \tag{3}$$

where f(a/W) is a non – dimensional function, given by:

$$f\left(\frac{a}{W}\right) = 6\sqrt{\frac{a}{W}}\,\frac{\left[1.99 - \frac{a}{W}\left(1-\frac{a}{W}\right)\left(2.15 - 3.93\frac{a}{W} + 2.7\left(\frac{a}{W}\right)^2\right)\right]}{\left(1+2\frac{a}{W}\right)\left(1-\frac{a}{W}\right)^{3/2}} \tag{4}$$

Where, P_Q is the force acting on the specimen; B is the specimen thickness; W is the specimen height; A is the crack length and S is the span length.

In order to validate the result obtained according to these test methods, the following size criteria must be satisfied:

$$a, B, (W - a) \geq 2.5\left(\frac{K_Q}{\sigma_{ys}}\right)^2 \tag{5}$$

where, σ_{ys} is the yield stress of the material for the temperature and loading speed of the test.

If condition (5) is satisfied, the critical stress intensity factor, K_{IC}, is considered to be equal to the calculated stress intensity factor, K_Q, so:

$$K_{IC} = K_Q \tag{6}$$

A. Static Fracture Toughness Tests of Rigid PUR Foam

Experimental tests for determining the static fracture toughness were made in the Strenght of Materials Laboratory, Faculty of Mechanical Engineering from Timisoara using a tension – compression Zwick/Roell 005 testing machine of 5 kN, (Fig. 27). Tests were performed at room temperature, 20±2 ℃, using specimens with the shape and dimensions shown in Fig. 28. For determining the fracture toughness of materials under investigation, notched specimens loaded in three – point bending were experienced. In the experimental program, rigid PU foams with 40 and 140 kg/m^3 were used. Fig. 29 presents the shape of the specimens tested. Both specimens and notches were cut from the same rectangular plate with a blade thickness of 0.6 mm.

Fig. 27 The 5 kN Zwick Roell 005 testing machine used for 3PB tests

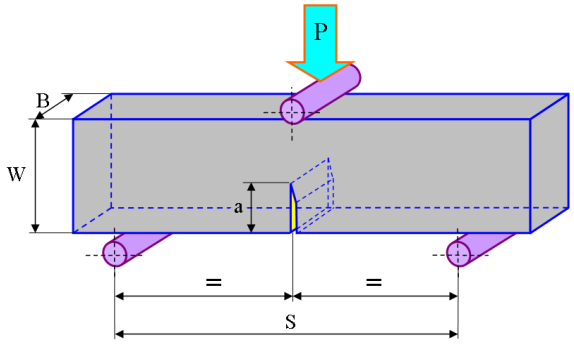

Fig. 28 Shape and dimensions of specimens used in the 3PB tests

Fig. 29 Specimens used in the three – point bending tests

The specimens were subjected to static three – point bending (3PB). The loading speed was 2 mm/min for determining the influence of loading direction, and a speed of 2, 20, 200 and 400 mm/min for determining the influence of loading speed. For each type of test, 5 specimens were used, and the tests were performed according to ASTM D 5045 – 99 (*Standard Test Methods for Plane – Strain Fracture Toughness and Strain Energy Release Rate of Plastic Materials*) [38] and in fact, it was taken into account that the load must act exactly on the notch direction.

1) Influence of loading speed

According to the influence of loading speed, the mean values of the fracture toughness obtained from the experimental tests for rigid polyurethane foam with 140 kg/m^3 density are listed in Table 7.

TABLE 7 MEAN VALUE OF THE MECHANICAL CHARACTERISTICS FOR ANALYSED FOAMS AFTER 3PB TESTS

Density [Kg/m^3]	Samples dimensions				Loading speed [mm/min]	Critical load [N]	Fracture toughness [MPa m$^{0.5}$]	$2.5\left(\frac{K_Q}{\sigma_{ys}}\right)^2$
	Width [mm]	High [mm]	Span length [mm]	Crack length [mm]				
140	13.9	24.9	100	12.5	2	34.70	0.156	7.9
	13.1	25.0			20	30.64	0.149	6.9
	14.6	25.1			200	28.50	0.137	4.7
	12.8	24.9			400	25.06	0.130	4.9

Fig. 30 presents the load – displacement curves for the studied foam and Fig. 31 shows the variation of fracture toughness versus loading speed.

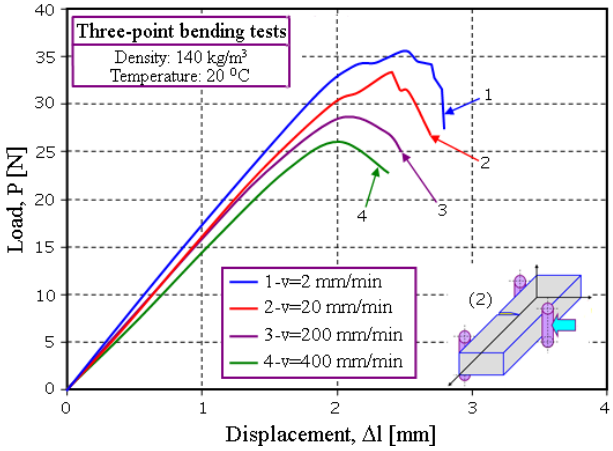

Fig. 30 Load-displacement curves for effect of loading speed

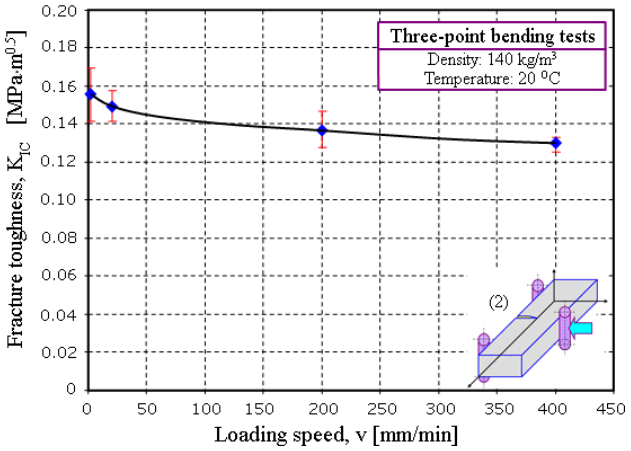

Fig. 31 Variation of fracture toughness versus loading speed

2) Influence of loading direction

The fracture toughness of anisotropic foams depends on the direction in which the crack propagates. This is the best defined with two subscripts, the first indicating the normal to the crack plane, the second the direction of crack propagation [1]. Fig. 32 is shows the sampling of the 3PB specimens extracted from a rectangular SF plate, and Fig. 33 shows the influence of loading direction on the mechanical characteristics at 3PB.

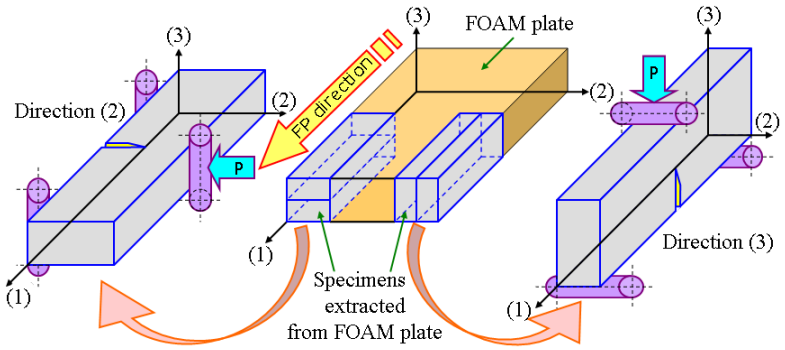

Fig. 32 The sampling of the 3PB specimens extracted from a rectangular SF plate

Loading direction emphasizes anisotropic behavior of the foam. The obtained mean values of fracture toughness are listed in Table 8. For all tested specimens, plane strain condition (3) was fulfilled and it can be observed from Table 8 that the variation of fracture toughness with load direction is insignificant (for this type of foam). It should be noted that brittle fracture was observed for all tested specimens. The linear – elastic behavior was confirmed during the tests when no cushioning occurs and no plastic deformations remain after the test [13].

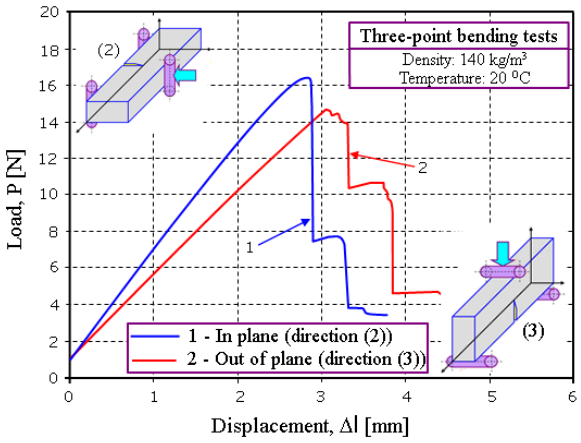

Fig. 33 Load-displacement curves for 3PB tests. Effect of loading direction

TABLE 8 MEAN VALUES OF FRACTURE TOUGHNESS VERSUS LOADING DIRECTION

Density [Kg/m^3]	Samples dimensions				Loading direction	Critical load [N]	Fracture toughness [MPa m$^{0.5}$]	$2.5\left(\frac{K_Q}{\sigma_{ys}}\right)^2$
	Width [mm]	High [mm]	Span length [mm]	Crack length [mm]				
40	25.5	49.4	180	25.0	(2)	16.4	0.0279	20.1
	25.1	50.2			(3)	14.2	0.0276	15.1

3) Size effect

Of particular interest is the fracture toughness of such foams because foam cracking weakens the structure's capacity for carrying load and absorbing energy [39]. In such case, the failure of the foam may be brittle, as revealed most clearly by the notched specimen tests of Zenkert [40] and Zenkert and Bäcklund [41], (and partly also suggested by holed panel tests of Olurin et al. [42] and Fleck et al. [43]). The brittle failure must generally be expected to exhibit a pronounced size effect [44, 45]. A size effect was revealed already in 1989 by Zenkert and Bäcklund's tests of notched foam beams. However, the size effect is important for extrapolating laboratory test data to very large structure. One of the most conclusive analytical descriptions of the size effect is presented by Zdenek et al. [46]. They presented simple formulae which would be easily usable in design and which could be exploited for conventional identification of material fracture properties from the measured size effect on the load capacities of notched foam specimens. They explored whether the energetic size effect law for quasi – brittle structures with large cracks, proposed by Bažant [47], extended by Bažant and Kazemi [48] and verified for concrete rocks, sea ice, ceramics, fiber composites and other quasi-brittle materials [44, 45], can be applied to rigid polyurethane foam and used for material parameter identification.

In this subsection the size effect was carried out on samples of polyurethane foam with a density of 40 kg/m3, with closed cells which are widely used as cores in sandwich panels. The static three point tests were performed in Laboratory from the Faculty of Building and Architecture at Lublin University of Technology. A 2 kN MTS static testing machine was used for bending tests, as shown in Fig. 34. In Fig. 35 are presented the sizes of specimens used in the experimental program. High dimensions samples were cut with a blade, and small dimensions samples were performed using a Secotom 10 cutting machine. All the specimens were cut from the same plate and had the same thickness B = 20 mm.

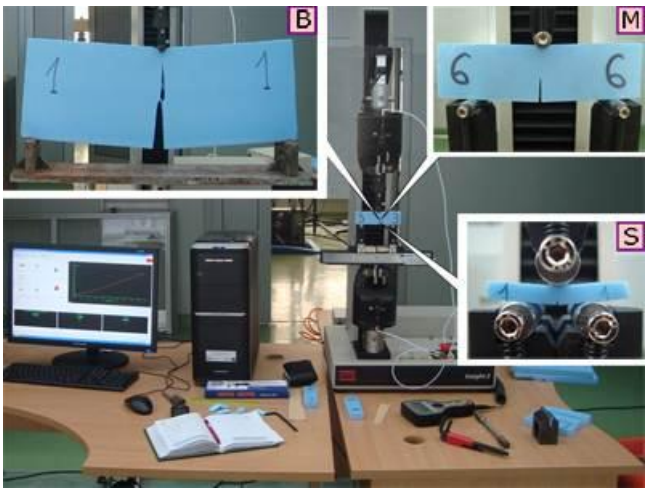

Fig. 34 A 2 kN MTS testing machine – seze effect

Fig. 35 Size effect samples

To determine the size effect of Mode I fracture toughness, specimens geometrically similar in two dimensions with length-to-width ratio 5:2 were selected. Their widths were W = 5.33; 36.89 and 256 mm, with a variation of span length S=13.33; 92.22 and 640 mm. Also, the notches having a length of 0.4W were cut with the two devices. Fig. 36 shown typical load – displacement curves obtained for different size specimens during the 3PB test. In this case, all the specimens have the same width B (20 mm), with different value of high, W, span length, S and crack length, a.

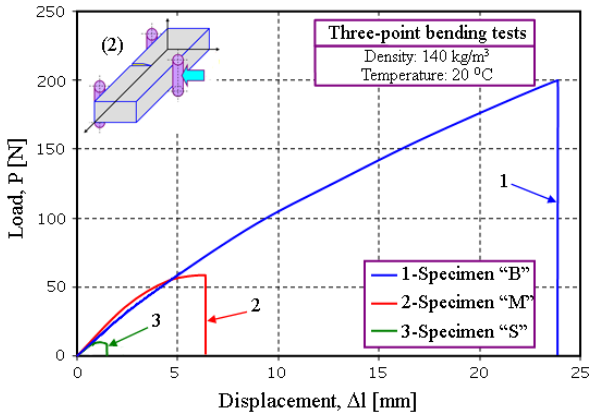

Fig. 36 Load – displacement curves. Size effect

In Table 9 are listed the main values of fracture toughness for foam with 40 kg/m^3 density, obtained from size effect tests.

TABLE 9 FRACTURE TOUGHNESS AND NOMINAL STRENGTH VALUES OBTAINED FROM THE SIZE EFFECT TESTS

Specimen Type	Density ρ [kg/m^3]	Specimen Dimensions				Loading Direction	Critical Load P [N]	Fracture Toughness K_{IC} [MPa m$^{0.5}$]	Nominal Strength σ_N [MPa]
		Width B [mm]	High W[mm]	Span Length S [mm]	Crack Length a [mm]				
"S"	40	20	5.33	13.33	2.13	(2)	8.71	0.047	0.323
							8.78	0.048	0.366
							9.12	0.049	0.345
							8.70	0.047	0.378
							8.64	0.047	0.362
"M"			36.89	92.22	14.76		43.54	0.090	0.221
							40.02	0.083	0.203
							43.60	0.090	0.221
							46.35	0.096	0.235
							50.85	0.105	0.258
"B"			256.00	640.00	102.40		217.11	0.170	0.091
							200.16	0.157	0.086
							212.51	0.166	0.090
							205.12	0.161	0.087
							215.95	0.169	0.091

Fig. 37 presents the variation of fracture toughness with crack length, a. It can be observed that the size effect has an influence on fracture toughness, which increases with increasing crack length.

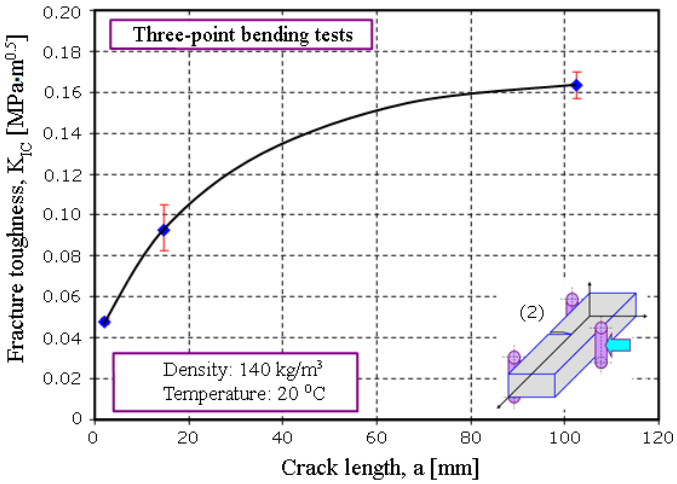

Fig. 37 Variation of K_{IC} with crack length

The size effect is defined as the dependence of the nominal strength, $\sigma_N = 3P_{max}S/(2BW^2)$, as a function of the characteristic specimen size W (here taken as the specimen width). Thus, the nominal strength is a parameter of the maximum load, having the dimension of stress. The size effect is best highlighted in a plot of Log (σ_N) versus log (W), presented in Fig. 38. If the failure of the foam obeyed linear elastic fracture mechanics (LEFM), the logarithmic size effect plot would have to be a straight line with the slope equal to –1/2 [46], shown by a dotted line in Fig. 38. A ductile behavior following the strength of material with no size effect would be a horizontal line $\sigma_N = \sigma_f$, where σ_f is the failure or plastic stress. The obtained experimental results are asymptotic to these approaches and they have the following form:

$$\sigma_N \propto \sigma_f (1+W/Wo)^{-1/2} \tag{6}$$

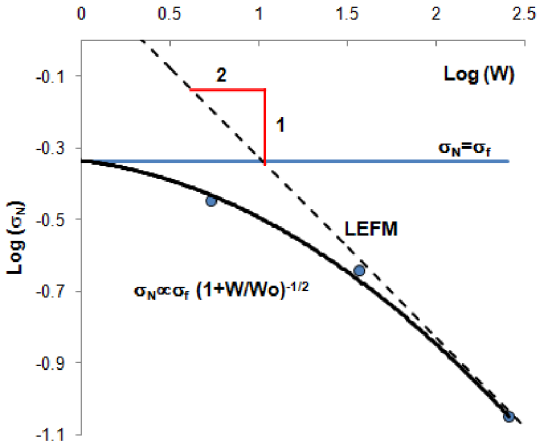

Fig. 38 Results of size effect tests of nominal strength of geometrically similar prismatic foam specimens with similar one-sided notch subjected to 3PB tests

Where, Wo represents the transitional size, which can be obtained by the intersection point of LEFM asymptote and the strength of materials horizontal line. For the investigated polyurethane foam $Wo \approx 10$ mm. This value was obtained using a failure stress $\sigma_f = 0.46$ MPa, determined experimentally on tensile tests.

For $Wo > 10$ mm the foam behavior is brittle, and the results are very close to the asymptotic line from LEFM approach, which means that, on the scale of the tests and of course on larger scales corresponding to structures, the material behaves in an almost brittle manner. For small specimens, a slight deviation occurs and the scaling should be done according with strength of plasticity approaches. Bazant [45] introduces also the brittleness number $\beta = W/Wo$ which allow to distinguish a brittle material $\beta \to \infty$ to a ductile (non – brittle) material $\beta \to 0$.

B. Dynamic Fracture Toughness Tests of Rigid PUR Foam

The principle of impact and instrumented impact tests of plastic materials are given in EN ISO 179 – 2:2000 [49] and Katthoff [50]. A KB Pruftechnik pendulum (Germany) was used for the instrumented impact tests (Fig. 39) with the following main characteristics: pendulum mass 2.04 kg, pendulum length 0.386 m, drop height 0.742 m, drop angle 157.32 º, pendulum energy 7.5 J, impact velocity 3.815 m/s. A four – channel data acquisition A/D card (AdLink NuDAQ PCI – 9812) was used for recording the load in time, and then the load – displacement curve was determined. A check for energy loses due to friction was performed prior to testing and it was found that the frictional loss was 0.059 J which represents 0.4% of the nominal energy of the pendulum 14.847 J. This fulfils the standard [49] condition that the energy loss due to friction should be less than 1%. Tests were performed at room temperature.

Fig. 39 Impact pendulum

Fig. 40 Specimens for impact tests

Three-point bending rigid polyurethane foam (40, 80, 120 and 140 kg/m^3 density) notched specimens shown in Fig. 40 were experimentally tested. Fig. 41 presents load – displacement curves for the above mentioned densities.

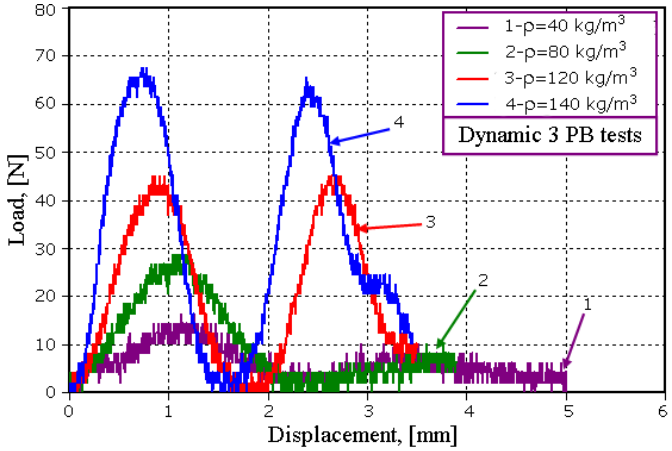

Fig. 41 Typical load- displacement curve from instrumented impact tests.

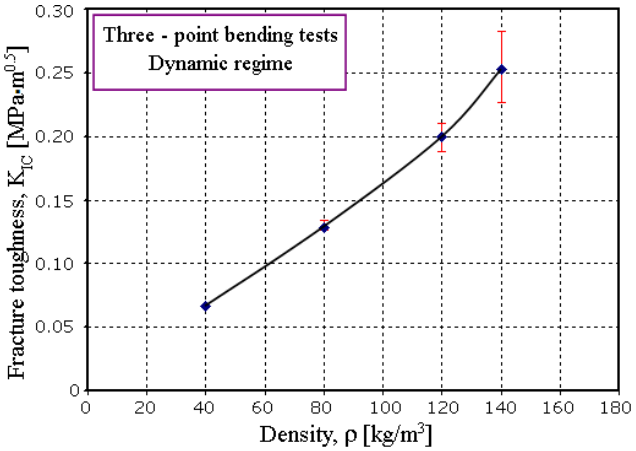

Fig. 42 Fracture toughness variation versus density

The dynamic fracture toughness was determined following the same procedure as in the case of static tests using relations (1) and (2). The mean values obtained in this case are presented in Table 10. These results were obtained in – plane loading direction – the direction (2) – at room temperature.

TABLE 10 MEAN VALUES OF DYNAMIC FRACTURE TOUGHNESS DEPENDING ON FOAM DENSITY

Density [kg/m^3]	Geometrical parameters				Critical load [N]	Fracture toughness [MPa m$^{0.5}$]	Energy [J]
	Width [mm]	High [mm]	Span length [mm]	Crack length [mm]			
40	13.48	25.39	100	12	14.360	0.066	0.084
80	13.91	25.54			29.120	0.129	0.110
120	13.04	25.00			40.606	0.200	0.140
140	13.02	25.70			54.600	0.253	0.196

According to the results presented in Table 10, Fig. 42 shows the fracture toughness variation depending on density. From this figure it can be seen that with increasing of density a significant increase of the fracture toughness is obtained, which means that the density plays a major role in determining the fracture parameters. Rigid polyurethane foams have a brittle fracture without plastic deformation as was mentioned above.

Fig. 43 presents the energy-time variation. In this case, also, the energy values increases with increasing of density.

C. Comparison between Static and Dynamic Fracture Toughness for 3PB Tests

Fig. 44 presents a comparison of the fracture toughness values obtained from both static and dynamic test. Experimental tests were performed on PUR foams with different densities using notched specimens loaded in 3-point bending at a 2 mm/min ($3.3 \cdot 10^{-5}$ m/s) loading speed for static tests, respectively 3.815 m/s for dynamic tests. Both in static and in dynamic regime the used temperature was 20 ℃.

As it can be seen from Fig. 44, rigid PUR foams behaves differently in the two regimes. The dynamic fracture toughness is about two times higher than static one.

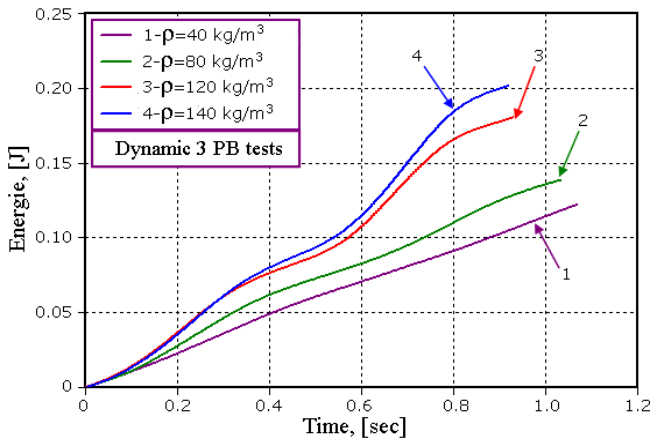

Fig. 43 Energy – time variation depending density

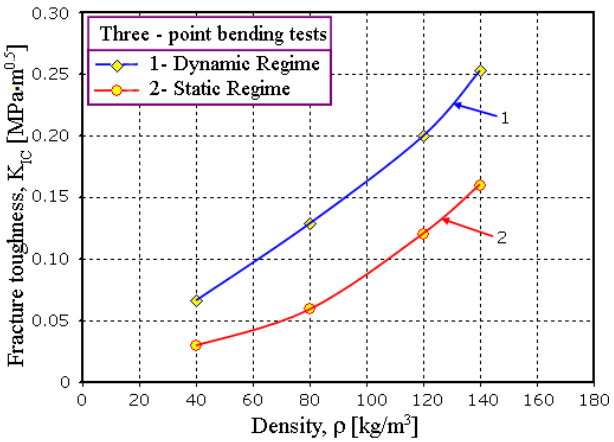

Fig. 44 Static and dynamic fracture toughness comparison

IV. MICROSTRUCTURAL ANALYSIS OF USED FOAMS

For analyzed foams, a microstructural analysis was made. The equipment used for microstructural characterization consists of Scanning Electron Microscope which is presented in Fig. 45. The analysis was done for both before (initial surface) and after (broken surface) compression and 3PB tests in the Strength of Materials Laboratory from the Lublin University of Technology, Poland.

Fig. 45 Scanning Electron Microscope used for microstructural analysis

Fig. 46 shows cell shapes before and after dynamic compression tests for foam with 140 kg/m^3 density. After compression tests the foam shows a total destruction of cells, which increases the stress delivered to an almost constant strain (known as densification). In the moment of densification, due to the filling of the gaps in the foam, this one acts almost like a solid material.

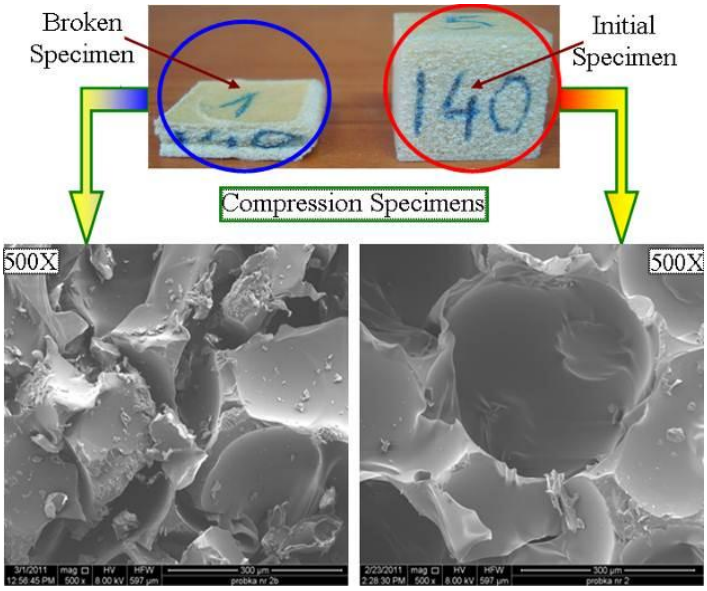

(a) fractured surface (b) initial surface

Fig. 46 SEM images of used PUR Foams

Initial and broken surfaces of rigid PUR foam used in 3PB experimental programs are presented in Fig. 47. Also, in the same figure is shown the cellular structure of foam having closed cell with ρ=40 and140 kg/m^3 density.

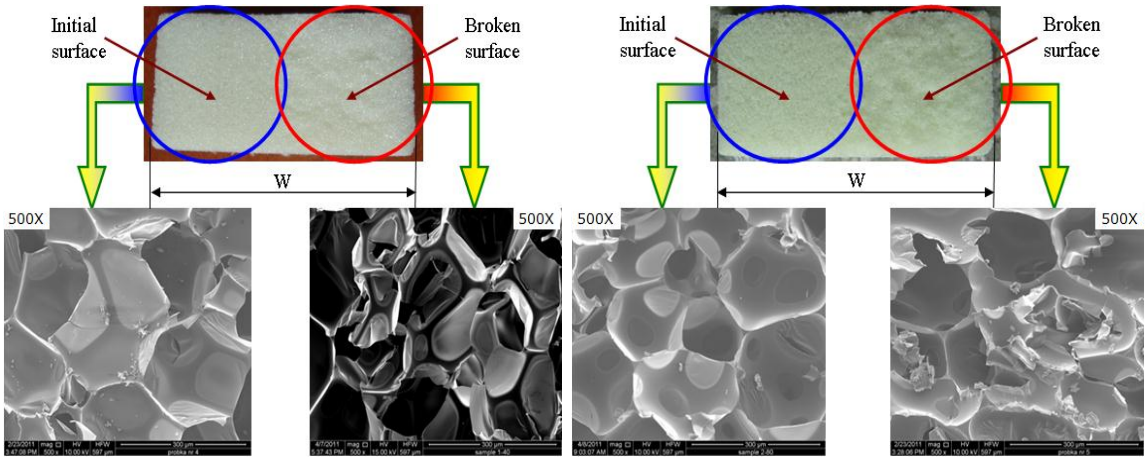

(a) 40 kg/m^3 density (b) 80 kg/m^3 density

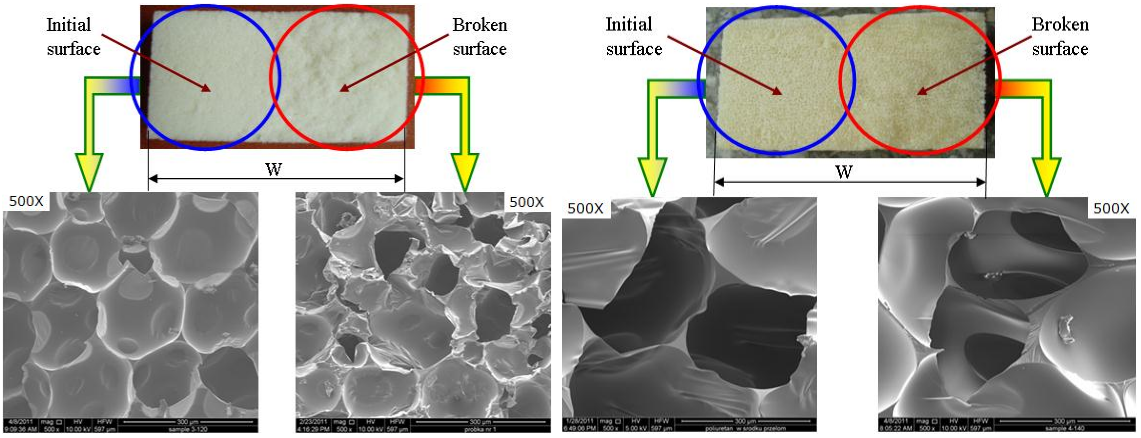

(c) 120 kg/m^3 density (d) 140 kg/m^3 density

Fig. 47 The microstructure of rigid polyurethane foams used for 3-point bending tests

All 3PB tested specimens show a quasi-brittle fracture without plastic deformations and cushioning.

V. CONCLUSIONS

Besides many other applications, polymeric cellular materials are used in the construction of wind turbine blade parts or entire sections. This book chapter presents the failure mechanisms in wind turbine blade with the focus on the core materials (rigid PUR foams). In this respect we made a mechanical characterization of rigid PUR foams under different loading conditions. This characterization of cores was done through static and dynamic tests with a focus on the influence of density (in the range of 40-200 kg/m^3), influence of loading speed (from $1.67.10^{-4}$ m/s – static tests to 6 m/s – impact tests), influence of forming plane (in-plane and out-of-plane loading direction), influence of temperature (from 20 ℃ to 100 ℃) and size effect on the mechanical properties. The most important mechanical properties which was studied are Young's modulus, yield stress, plateau stress, densification and fracture toughness.

After the experimental investigations, the following conclusions can be drawn:

D. For static and dynamic compression tests

- The experimental study presents a comparison of the stress-strain response in dynamic compression. It can easily be seen that with increasing of density we obtain a significant increase of mechanical properties, which means that the density has an important role in determining the dynamic compressive behavior.

- Loading speed has a little influence on mechanical properties in dynamic compression for low density of PUR foams (80 and 93 kg/m^3), while for high densities loading speed it has a major influence (200 kg/m^3). It can be observed that the biggest influence is obtained for linear – elastic region, yield stress and densification region.

- The loading direction has a major influence on the compressive mechanical properties in dynamic conditions, this parameter clearly showing the anisotropic aspect of foam. For an in – plane loading direction a constant plateau was obtained, while for out – of – plane load the plateau has a linear hardening (for the same foam density).

- From Fig. 11 it can be observed that cross-section shows a relatively small influence on the mechanical properties.

- According to the results presented in Fig. 19, it can be seen that at lowest temperatures (20 and 60°C) the behavior of foam is approximately the same, while at high temperature (100 ℃), foams show a major change in their properties.

- Also, the calculation of densification strain for rigid polyurethane foams was presented. The onset strain of densification is an important parameter in the design and modeling of cellular materials.

E. For static and dynamic fracture toughness tests

- This section presents influence of few parameters on fracture toughness of rigid PUR foams: influence of density, influence of loading speed, influence of forming plane and size effect.

- The values of fracture toughness for PUR foams are in the range of $10^{-3} – 10^{-1}$ MPa·m$^{0.5}$. Fracture toughness increase with increasing of density and decrease with increasing of loading speed.

- Loading direction emphasizes anisotropic behavior of the foam. For this type of PUR foam with 40 kg/m^3 density, the same fracture toughness was approximately obtained.

- Experimental investigations on size effect of closed-cell PUR foam of density 40 kg/m^3 were carried on 3-point bending specimens of different sizes, keeping constant the specimen thickness B=20 mm and ratio between crack length a and specimen width W: a/W = 0.4. A strong size effect in the closed – cell PUR foam (PUR 40) is experimentally demonstrated, representing the transition between strength of materials approach (with no size effect) and asymptotic case of linear elastic fracture mechanics. The size effect is also highlighted by the fracture toughness results, which increased with increasing specimen width and accordingly crack length. From the practical point of view and in order to determine the fracture toughness of this PUR foam, a minimum width size W_o=10 mm should be used, which represents approximately 33 cells (mean cell size for investigated foam was 0.3 mm). The size effect in foam is important for extrapolating laboratory tests data to very large structures, such as wind turbine blades. To summarize, the size effect presented in Fig. 38, demonstrates that the current design practice, in which the tensile failure of foam is generally predicted on the basis of strength criteria or plasticity, is acceptable only for small structural parts. In the case of large structural parts, the size effect must be taken into account, and linear elastic fracture mechanics concepts must be applied, especially in the presence of long cracks or large damage zones.

F. For Microstructural Analysis

Also at the end of this book chapter is shown a microstructural analysis for both before (initial surface) and after (broken surface) compression and three – point bending tests.

- After compression tests the foam shows a total destruction of cells, which increases the stress delivered to an almost constant strain (known as densification). In the moment of densification, due to the filling of the gaps in the foam, this one acts almost like a solid material, see Fig. 46.

- All 3PB tested specimens show a quasi – brittle fracture without plastic deformations and cushioning.

As a final conclusion we can say that one of the most significant parameter on the mechanical properties for cellular materials is the density. Hence, the mechanical properties of foams can be controlled, making them attractive in structural application requiring particular strength or stiffness to weight ratios. Cellular materials have plastic plateau and densification in compression, while in tensile they are quasi-brittle.

ACKNOWLEDGMENTS

This work was supported by the strategic grant POSDRU 6/1.5/S/13 (2008) of the Ministry of Labour, Family and Social Protection, Romania, co–financed by the European Social Fund – Investing in People and by a grant of the Romanian National Authority for Scientific Research, CNCS – UEFISCDI, project PN-II-ID-PCE-2011-3-0456, contract number 172/2011.

REFERENCES

[1] L.J Gibson, M.F Ashby, Cellular solids. Structure and properties, Second edition, published by the Press Syndicate of Cambridge, 1997.

[2] E. Linul, L. Marşavina, A. Cernescu, Assessment of sandwich beams using failure mode maps, 16th International Conference on Composite Structures, Porto, Portugal, Jun. 2011.

[3] G. Ji, Z. Ouyang and G. Li, Debonding and impact tolerant sandwich panel with hybrid foam core, Comp. Struct. 103, 2013, 143-150.

[4] B. Yang and D. Sun, Testing, inspecting and monitoring technologies for wind turbine blades: A survey, Renewable and Sustainable Energy Reviews 22, 2013, 515-526.

[5] S. Ahmed and D. Izhar-ul-Haq, Wind Blade Material Optimization, Advances in Mechanical Engineering, vol. 2, no. 4, Dec., 2012.

[6] C. Sicot, P. Devinant, S. Loyer and J. Hureau, Rotational and turbulence effects on a wind turbine blade. Investigation of the stall mechanisms, Journal of Wind Engineering and Industrial Aerodynamics 96, 2008, 1320-1331.

[7] C. Kong, T. Kim, D. Han and Y. Sugiyama, Investigation of fatigue life for a medium scale composite wind turbine blade, International Journal of Fatigue 28, 2006, 1382-1388.

[8] J. Yang, C. Peng, J. Xiao, J. Zeng, S. Xing, J. Jin and H. Deng, Structural investigation of composite wind turbine blade considering

structural collapse in full-scale static tests, Composite Structures 97, 2013, 15-29.

[9] D. S. Zarouchas, A. A. Makris, F. Sayer, D. Van Hemelrijck and A. M. Van Wingerde, Investigations on the mechanical behavior of a wind rotor blade subcomponent, Composites: Part B 43, 2012, 647-654.

[10] C. P. Chen and T. Y. Kam, Failure Analysis of Small Composite Sandwich Turbine Blade Subjected to Extreme Wind Load, Procedia Engineering 14, 2011, 1973-1981.

[11] A. Mirzapour, M. H. Beheshty and M. Vafayan, The response of sandwich panels with rigid polyurethane foam cores under flexural loading, Iranian Polymer Journal, 14 (12), 2005, 1082-1088.

[12] C.S. Lee and D.G. Lee, Co-cure method for foam sandwich composite manufacture, Comp. Struc., 66, 2004, 231-238.

[13] M. Avalle, G. Belingardi and R. Montanini, Characterization of polymeric structural foams under compressive impact loading by means of energy-absorption, International Journal of Impact Engineering 25, 2001, 455-472.

[14] M. Avalle, G. Belingardi and G. Ibba, Mechanical models of cellular solids: Parameters identification from experimental tests, International Journal of Impact Engineering 34, 2007, 3-27.

[15] M. C. Saha, H. Mahfuz, U. K. Charavarthy, M. Uddin, M. E. Kabir and S. Jeelani, Effect of Density, Microstructure, and Strain Rate on Compression Behavior of Polymeric Foams, Materials Science and Engineering, A406, 2005, 328-336.

[16] S. Ouellet, D. Cronin and M. Worswick, Compressive Response of Polymeric Foams Under Quasi-static, Medium, and High Strain Rate Conditions, Polymer Testing, 25, 2006, 731-743.

[17] F. Ramsteiner, N. Fell and S. Forster, Testing the deformation behaviour of polymer foams, Pol. Test., 20, 2001, 661-670.

[18] E. Linul, L. Marsavina and A. V. Cernescu, Effect of loading speed, the direction of formation and density of rigid polyurethane foams subjected to compression, Acta Tehnica Napocensis, Series: Mech. Eng. Mat. Sci. 53, 2010, 311-316.

[19] Q. M. Li, I. Magkiriadis, J. Harrigan, Compressive strain at the onset of densification of cellular solids, J of Cell Plastics, 42, 2006, 371.

[20] Z. H. Tu, V. P. W. Shim, and C. T. Lim, Plastic deformation modes in rigide polyurethane foam under static loading, International Journal of Solids and Structures 38, 2001, 9267-9279.

[21] A. Ajdari, Mechanical behaviour of cellular structures a finite element study, Master on Science in Mechanical Engineering, Northeastern Universty, boston, Massachusetts, Apr., 2008.

[22] ASTM D1621 – 00, Standard Test Method for Compressive Properties of Rigid Cellular Plastics.

[23] T.G. Nieh, K. Higashi and J. Wadsworth, Effect of Cell Morphology on the Compressive Properties of Open-cell Aluminum Foam. Material Science and Engineering, A283 (1-2), 2000, 105-110.

[24] A. Paul and U. Ramamurthy, Strain rate Sensitivity of a Closed-cell Aluminum Foam, Mat. Sci. and Eng., A281 (1), 2000, 1-7.

[25] K. C. Chan, L. S. Xie, Dependency of Densification Properties on Cell Topology of Metal Foams. Scripta Mat., 48 (8), 2003, 1147-1152.

[26] M. Vural and A. G. Ravich, Microstructural Aspects and Modeling of Failure in Naturally Occurring Porous Composites. Mechanics of Materials, 35 (3-6), 2003, 523-536.

[27] N. Tuncer, G. Arslon, Designing Compressive properties of titanium foams. J. of Material Science, 2009, 1477-1484.

[28] L. Marsavina, T. Sadowski, D. M. Constantinescu and R. Negru, Polyurethane Foams Behaviour. Experiments versus Modeling. Key Engineering Materials, vol. 399, 2008, 123-130.

[29] T. Wiydia, C. W. Macosko, Nanoclay-Modified Rigid Polyurethane Foams, J. of Macromolecular Sci., Part B: 44, 2005, pp. 897-908.

[30] H. Altenbach and A. Ochsner, Cellular and Porous Materials in Structures and Proceses, CISM Courses and Lectures, vol. 521. Ed. Springer Wien New York, Udine, 2010.

[31] A. McIntyre, G. Anderson, Fracture properties of rigid PU foam over a range of densities, Polymer, 20, 1979, pp. 247-253.

[32] M. Danielsson, Toughened rigid foam core material for use in sandwich construction, Cell. Pol., 15, 1996, pp. 417-435.

[33] M. Burman, Fatigue crack initiation and propagation in sandwich structures, Report no. 98-29, Stockholm, 1998.

[34] G.M. Viana and L. A. Carlsson, Mechanical Properties and Fracture Characterization of Cross-Linked PVC Foams, J. Sandw Struct Mater, 4, 2002, pp. 91-113.

[35] Md.E. Kabir, M. C. Saha and S. Jeelani, Tensile and fracture behavior of polymer foams, Mat. Sci. and Eng. A, 429, 2006, pp. 225-235.

[36] L. Marsavina, E. Linul, Fracture toughness of polyurethane foams, Experimental versus micromechanical models, Fracture of Materials and Structures from Micro to Macro Scale. 18th European Conf. on Fracture, Dresden, Germany, Aug. 30-Sep. 03, 2010.

[37] E. Linul, L. Marsavina and A. Cernescu, Determination of fracture toughness for cellular materials such as polyurethane foams, Fracture Mechanics. 15th National Symposium National on Fracture Mechanics, Ed. Universitatii Petrol-Gaze Ploiesti and Ed. Universitatii "Lucian Blaga" from Sibiu, 6-7 Nov, 2009, Sibiu, pp. 15-22.

[38] ASTM D 5045-99 Standard Test Methods for Plane-Strain Fracture Toughness and Strain Energy Release Rate of Plastic Materials.

[39] L. Marsavina, Fracture mechanics of cellular solids, in Cellular and porous materials in structures and processes, Springer, 2010, 1-33.

[40] D. Zenkert, PVC sandwich core materials: fracture behaviour under mode II and mixed mode loading, Mat Sci Eng. 108, 1989, 233-240.

[41] D. Zenkert, J. Bäcklund, PVC sandwich core materials: mode I fracture toughness. Comp. Sci. Tech. 34, 1989, 225-242.

[42] O. B. Olurin, N. A. Fleck, M. F. Ashby, Tensile and compressive failure of notched cellular foams, Adv Eng Mat 3 (1–2), 2001, 55-58.

[43] N. A. Fleck, O. B. Olurin, C. Chen, M. F. Ashby, The effect of hole size upon the strength of metallic and polymeric foams, J. of the Mech. and Phys. of Sol. 49, 2001, 2015-2030.

[44] Z. P. Bažant, J. Planas, Fracture and size effect in concrete and other quasi-brittle materials, CRC Press, Boca Raton and London (Sections 9.2 and 9.3), 1998.

[45] Z. P. Bažant, Scaling of Structural Strength, Hermes-Penton, London, 2002.

[46] P. Zdenek, Z. P. Bažant, Z. Yong, Z. Goangseup, M. D. Isaac, Size effect and asymptotic matching analysis of fracture of closed-cell polymeric foam, Int. J. of Sol. and Struc. 40, 2003, 7197-7217.

[47] Z. P. Bažant, Size effect in blunt fracture: Concrete, rock, metal, J. of Eng. Mech. ASCE 110, 1984, 518-535.

[48] Z. P. Bažant, M. T. Kazemi, Determination of fracture energy, process zone length and brittleness number from size effect, with application to rock and concrete, Int. J. of Fract. 44, 1990, 111-131.

[49] EN ISO 179–2:2000. Plastics – Determination of Charpy impact properties. Part 2: instrumented impact test.

[50] J. F. Kalthoff, Characterization of the dynamic failure behaviour of a glass – fiber / vinyl – seter at different temperatures by means of instrumented Charpy impact testing, Comp. Part. B 35, 2004, 657–663.

Emanoil LINUL was born in Năsăud, Romania on November 12, 1984. He is an Assistant Lecturer in the Department of Mechanics and Strength of Materials at POLITEHNICA University of Timisoara, Romania. Dr. Linul obtained his Ph.D. Degree in the Engineering Science field under the supervision of Prof. Liviu Marşavina – Thesis Title: "Study of the Influence Factors Affecting the Mechanical Properties of Rigid Polyurethane Foams", September 9, 2011. Throughout the last year of his Ph.D. Thesis he worked with experienced researchers, i.e. Prof. Tomasz Sadowski and his team from Lublin University of Technology, Poland.

In addition to teaching activities, Dr. Linul is a member of Romanian Society for Experimental Stress Analysis (ARTENS) and of Romanian Association for Fracture Mechanics (ARMR), since 2009. Currently, he is a Research Assistant and working as a scientist in the National Grant "Micro-mechanical modeling of cellular materials with refinements on fracture and damage", where he is investigating cellular materials (rigid PU foams) behavior.

His main research interests include: (i) experimental characterization of cellular materials (compression, tensile, shear, bending and fracture tests); (ii) development of micro-mechanical models to estimate mechanical properties of cellular materials; (iii) implementation of constitutive material models in Finite Element Analysis; (iv) investigation of the size and notch effects on cellular materials using Theory of Critical Distance; (v) evaluation of the behavior of cellular materials under dynamic (impact, fatigue and energy absorption) loading; (vi) investigation of the effect of micro-structural damage on the mechanical properties of cellular materials using Digital Image Correlation (DIC) and thermography systems.

Also, he recently collaborated with Dr. Jaroslav Kovacik from Slovak Academy of Science, Bratislava, Slovakia on mechanical behavior of aluminum foams field. As a result of research work, since 2010 he has published more than 25 papers in journals, publications and book conferences of which 15 in the ISI circuit (7 papers in ISI Journals and 8 papers in ISI Proceedings).

Liviu MARŞAVINA was born in Anina, Romania on September 23, 1963. He is a Professor in the Department of Mechanics and Strength of Materials at POLITEHNICA University of Timisoara (UPT), Romania, since 2006 and was Head of Strength of Materials Department of UPT (2008-2011). With a Ph.D. Thesis entitled "Numerical Methods Used in Fracture Mechanics" and with an experience in this field, he has published more than 80 scientific/technical papers.

Professor Marsavina attended several specialized courses of which the most important are: (i) Course "Optical Methods in Solid Mechanics", Loughborough University, UK, March-June 2000; (ii) PECO Workshop IE-W03 "Best Practice of Advanced Fracture Assessment", Petten, NEDERLAND, April 2003 and (iii) Advanced course: "Multi-scale Modelling of Damage and Fracture Processes in Composite Materials" at International Centre for Mechanical Sciences, CISM Udine, ITALY, May 2004.

Dr. Marsavina has different positions in international research environment: (i) Postdoctoral researcher at Loughborough University, UK in 2000; (ii) Research Associate at the University of Sheffield, UK from 2001-2002; (iii) Marie Curie Experienced Researcher at Lublin University of Technology, Poland from 2007-2008.

Besides teacher position he has the following positions: (i) member of the CSUD (Council of Doctoral Studies); (ii) Ph.D. supervisor from 2007; (iii) member in the committee for Ph.D. examination/defence at UPT, Politehnica University of Bucharest, Lille University (France), Loughborough University (UK); (iv) member in the CNTDCU (National Council for Titles, Diplomas and University Certificates) of Romanian Ministry of Education; (v) member in the CNCS (National Council of Scientific Research) of Romanian Ministry of Education; (vi) member of ARTENS (Romanian Society for Experimental Stress Analysis); (vii) member of SIAC (Romanian Society for Computer – Aided Engineering); (viii) member and vice-president of ARMR (Romanian Association for Fracture Mechanics); (ix) member of AGIR (Romanian Engineering General Association); (x) member of EU – RA (European Research Associates) and (xi) member of ESIS (European Structural Integrity Society).

Dr. Marsavina is co-editor of Bulletin of Romanian Association of Fracture Mechanics and member in Advisory Board of International Journal of Structural Integrity. Also, he is reviewer for the following journals: Fatigue and Fracture of Engineering Materials and Structures (Blackwell Ltd.) from 2001; Journal of Sound and Vibration (Elsevier) from 2006; Computational Material Science (Elsevier) from 2006; Construction and Building Materials (Elsevier) from 2007; International Journal of Solids and Structures (Elsevier) from 2009; Mechanical Research Communications (Elsevier) from 2009; Mechanics of Advanced Materials and Structures (Taylor and Francis) from 2009; Journal of Mechanical Science and Technology (Springer) from 2010; Engineering Fracture Mechanics (Elsevier) from 2010 and Frattura ed Integrità Strutturale (Gruppo Italiano Frattura) from 2012.

Research interests of Dr. Marsavina are: (i) Fracture mechanics and structural integrity; (ii) mechanical testing; (iii) fatigue of materials; (iv) composite materials including cellular materials; (v) experimental stress analysis (photoelasticity, thermoelasticity, Digital Image Correlation) and (vi) numerical stress analysis for evaluating the fracture parameters.

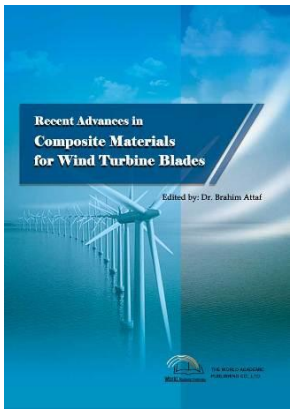

Recent Advances in Composite Materials for Wind Turbine Blades
Edited by Dr. Brahim Attaf

ISBN 978-0-9889190-0-6

Hard cover, 232 pages

Publisher: The World Academic Publishing Co. Ltd.

Published in printed edition: 20, December 2013

Published online: 20, December 2013

This book of science and technology provides an overview of recent research activities on the application of fibre-reinforced composite materials used in wind turbine blades. Great emphasis was given to the work of scientists, researchers and industrialists who are active in the field and to the latest developments achieved in new materials, manufacturing processes, architectures, aerodynamics, optimum design, testing techniques, etc.. These innovative topics will open up great perspectives for the development of large scale blades for on- and off-shore applications. In addition, the variety of the presented chapters will offer readers access to global studies of research & innovation, technology transfer and dissemination of results and will respond effectively to issues related to improving the energy efficiency strategy for 2020 and the longer term.

How to cite this book chapter

Linul E. and Marsavina L. (2013). Mechanical Characterization of Rigid PUR Foams Used for Wind Turbine Blades Construction, *Recent Advances in Composite Materials for Wind Turbines Blades*, Dr. Brahim Attaf (Ed.), ISBN 978-0-9889190-0-6, WAP-AMSA, Available from: http://www.academicpub.org/amsa/chapterInfo.aspx

World Academic Publishing - Advances in Materials Science and Applications